energies

MDPI

Article

Device Performance Improvement of Double-Pass Wire Mesh Packed Solar Air Heaters under Recycling Operation Conditions

Chii-Dong Ho *, Hsuan Chang, Chun-Sheng Lin, Chun-Chieh Chao and Yi-En Tien

Energy and Opto-Electronic Materials Research Center, Department of Chemical and Materials Engineering, Tamkang University, Tamsui, New Taipei 251, Taiwan; nhchang@mail.tku.edu.tw (H.C.); cicadas0908@hotmail.com (C.-S.L.); tokyo363@gmail.com (C.-C.C.); tienyien@gmail.com (Y.-E.T.)

* Correspondence: cdho@mail.tku.edu.tw; Tel.: +886-2-2621-5656 (ext. 2724); Fax: +886-2-2620-9887

Academic Editor: Timothy Anderson

Received: 18 December 2015; Accepted: 18 January 2016; Published: 22 January 2016

Abstract: The improvement of device performance of a recycling solar air heater featuring a wire mesh packing was investigated experimentally and theoretically. The application of the wire mesh packing and recycle-effect concept to the present study were proposed aiming to strengthen the convective heat-transfer coefficient due to increased turbulence. Comparisons were made among different designs, including the single-pass, flat-plate double-pass and recycling double-pass wire mesh packed operations. The collector efficiency of the recycling double-pass wire mesh packed solar air heater was much higher than that of the other configurations for various recycle ratios and mass flow rates scenarios. The power consumption increment due to implementing wire mesh in solar air heaters was also discussed considering the economic feasibility. A fairly good agreement between theoretical predictions and experimental measurements was achieved with an analyzed error of 1.07%–9.32%.

Keywords: wire mesh packing; heat-transfer efficiency; double-pass; recycling; solar air heater

1. Introduction

Various solar air heater configurations have been implemented to enhance collector efficiency compared to a simple flat-plate device consisting of glass covers, an absorber plate and air flow channels. Razika *et al.* [1] and Al-Kayiem and Yassen [2] discussed the effect of the inclination angle on the absorption-convection heat transfer mechanism in a solar air collector. El-Sebaii and Al-Snani [3] investigated the effects of using absorber plates coated with various selective coating materials on the collector performance. Vaziri *et al.* [4] presented the collector performances of new solar air collector designs having different inner collector colors. Many improved devices were designed taking into account the design parameters for strengthening the convective heat-transfer coefficient [5], enlarging heat-transfer area [6], and increasing flow turbulence [7]. Several investigators have confirmed the technical feasibility of the recycle-effect application to heat transfer devices and reactors. Ho *et al.* [8,9] derived the theoretical formulations of the recycle-effect concept to heat and mass transfer through a parallel-plate channel with recycle. Fudholi *et al.* [10] developed the improvement potential of the solar collector based on energy and exergy analyses. Singh and Dhiman [11] proposed an analytical study to predict the thermal and thermohydraulic efficiencies of recycling double-pass packed bed solar air collectors. Garg *et al.* [12] extended solar air heater operation to multiple-pass operations. Enhancement of convective heat-transfer coefficients was achieved by increasing the intensity of the turbulence in recycling solar air collectors with double-pass [13] and multi-pass [14] operations. In this work a new solar air heater design adopting a wire mesh packed double-pass design under recycling

operation, as shown in Figures 1 and 2 is proposed and studied. There are two purposes in the present study: first, to obtain theoretical predictions and to obtain the experimental results for the recycling double-pass wire mesh packed solar air heater; and second, to study the effects of the recycle ratio and air mass flow rate on the heat-transfer efficiency enhancement and to make an economic consideration of both heat-transfer efficiency improvement and power consumption increment.

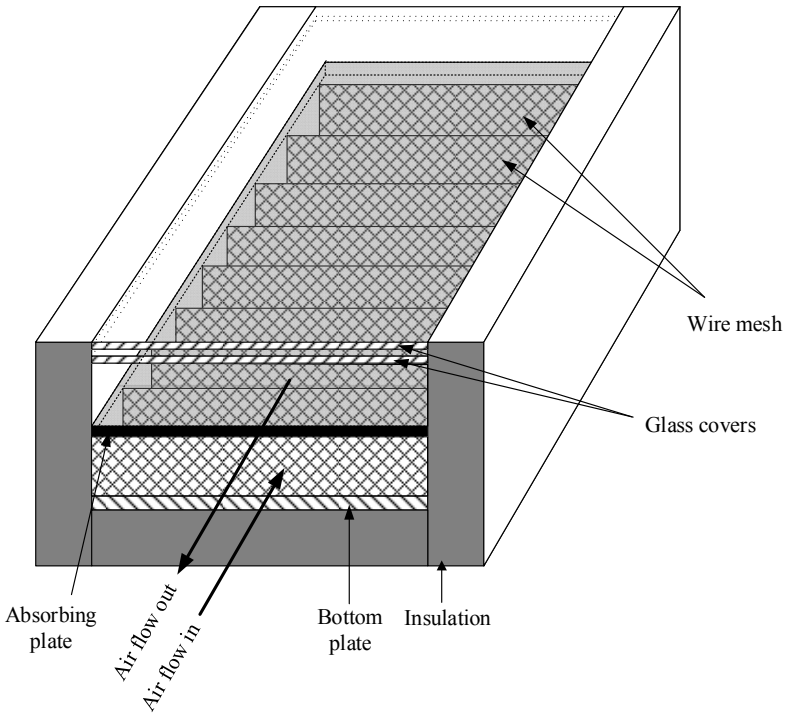

Figure 1. Configuration of a recycling double-pass solar air heater.

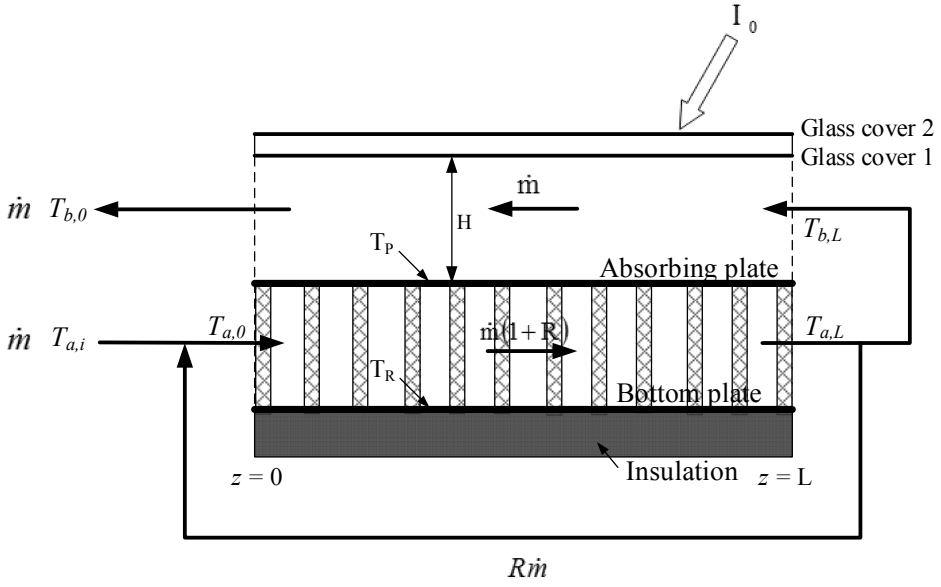

Figure 2. A double-pass solar air heater with internal attached wire mesh.

2. Temperature Distributions

Before entering the lower subchannel, the inlet air mass flow rate and inlet temperature of $\dot{m}$ and $T_{a,i}$ is premixed with the recycling air flow $R\dot{m}$ exits from the lower subchannel with the outlet

temperature $T_{a,L}$. A schematic configuration is depicted in Figure 1 while the air flow arrangement is shown in Figure 2.

By following the similar mathematical treatment and experimental studies performed in our previous work [15], except instead for the wire mesh packing, the analytical solutions of the temperature distributions of the flowing air in the lower and upper subchannels can be obtained in dimensionless form as:

$$T_a(\xi) = C_1 e^{Y_1 \xi} + C_2 e^{Y_2 \xi} + \frac{B_3 B_4 - B_1 B_6}{B_1 B_5 - B_2 B_4} + T_s \tag{1}$$

$$T_b(\xi) = \frac{Y_1 - B_5}{B_4} C_1 e^{Y_1 \xi} + \frac{Y_2 - B_5}{B_4} C_2 e^{Y_2 \xi} - \frac{B_5 (B_3 B_4 - B_1 B_6)}{B_4 (B_1 B_5 - B_2 B_4)} - \frac{B_6}{B_4} + T_s \tag{2}$$

For the definitions of B_i, G_i, M_i, Y_i, C_i, F_i and I_i readers are referred to the Appendix. The outlet temperature of $T_{b,0}$ can be calculated from Equation (2):

$$T_b(0) = T_{b,0} = \frac{Y_1 - B_5}{B_4} C_1 + \frac{Y_2 - B_5}{B_4} C_2 - \frac{B_5 (B_3 B_4 - B_1 B_6)}{B_4 (B_1 B_5 - B_2 B_4)} - \frac{B_6}{B_4} + T_s \tag{3}$$

Estimation of the useful energy gained by the flowing air was obtained from the energy balance on the lower subchannel, upper subchannel and whole solar air heater with the known inlet and outlet temperatures, respectively:

$$Q_u = \dot{m} (1 + R) C_p (T_{a,L} - T_{a,0}) + \dot{m} C_p (T_{b,0} - T_{b,L}) \tag{4}$$

or:

$$Q_u = \dot{m} C_p (T_{a,L} - T_{a,i}) + \dot{m} C_p (T_{b,0} - T_{b,L}) = \dot{m} C_p (T_{b,0} - T_{a,i}) \tag{5}$$

For simplicity, the collector efficiency η_W of the double-pass wire mesh packed solar air heater with external recycle was obtained from the actual useful energy gained by the airflow and the incident solar radiation as:

$$\begin{aligned} \eta_W &= \frac{Q_u \text{ (Useful gain of energy carried away by air)}}{I_0 A_c \text{ (Total solar radiation incident)}} \\ &= \frac{\dot{m} C_p (T_{b,0} - T_{a,i})}{I_0 A_c} = \frac{I_0 \tau_g^2 \alpha_p - U_L (T_{p,m} - T_s)}{I_0} \end{aligned} \tag{6}$$

Equating and rearranging the terms of Equation (6), the average absorber temperature was obtained as:

$$T_{p,m} = T_s + (I_0 \tau_g^2 \alpha_p / U_L) - \frac{\dot{m} C_p (T_{b,0} - T_{a,i})}{A_c U_L} = T_s + (I_0 / U_L)(\tau_g^2 \alpha_p - \eta_W) \tag{7}$$

3. Experimental Studies

The experimental setup of the recycling double-pass wire mesh packed solar air heater with subchannel width, length and height of 0.3 m, 0.3 m and 0.05 m, respectively, is shown in Figure 3. One set of heat sources with on/off switch consisted of 14 energy supplies (110 V, 125 W) situated 0.15 m above the glass cover, and the insolation was measured and recorded with instantaneous solar radiation meter (Model No. 455, the Epply Laboratory Inc., St. Paul, MN, USA). Temperatures of flowing air in the interior and at the inlet and outlet of the collector and the air mass flow rate were measured while the ambient temperature was regulated using an air conditioner. Before entering the lower subchannel, the airflow with mass flow rate $\dot{m}$ and temperature $T_{a,i}$ will premix the air flow exiting from the lower subchannel with $R\dot{m}$ and $T_{a,L}$ which is regulated by means of a valve situated at the end of the lower subchannel. Twenty pieces of the wire mesh were welded into the lower subchannel using a mesh interval of 0.015 m and mesh pitch of 0.003 m. The experimental runs

were carried out to supply the ambient air by a blower (Teco 3 Phase Induction Motor, Model BL model 552, Redmond Co, Owosso, MI, USA) which was measured by an anemometer (Kanmax Japan Inc., Osaka, Japan). By substituting the specified values into the appropriate equations, the theoretical predictions were obtained and also presented graphically in Figures 4 and 5 for comparisons between different devices.

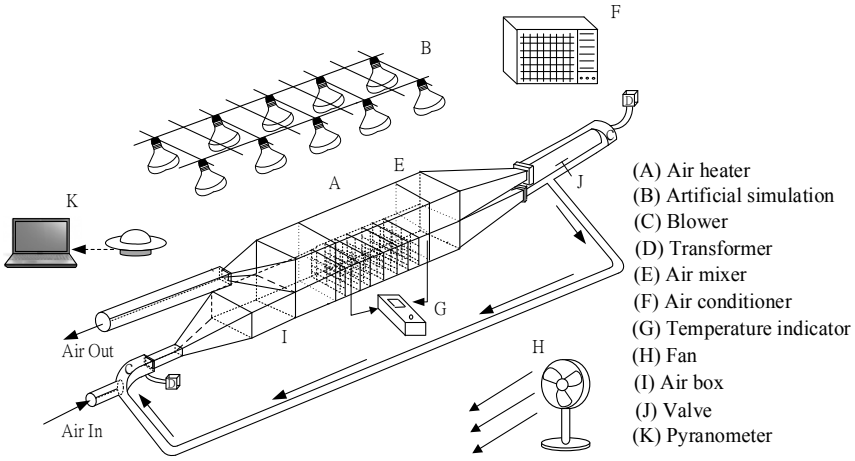

Figure 3. Schematic diagram of a double-pass solar air heater with artificial simulation.

4. Results and Discussion

Moffat [16] determined the precision analysis of each individual measurement directly from the experimental run as follows:

$$S_{\eta_{\exp}} = \left\{ \sum_{i=1}^{N_{\exp}} \frac{\left(\eta_{\exp,i} - \overline{\eta}_{\exp,i}\right)^2}{N-1} \right\}^{1/2} \tag{8}$$

and the mean value of resulting uncertainty of experimental runs was defined by:

$$S_{\overline{\eta}_{\exp}} = \frac{S_{\eta_{\exp}}}{\sqrt{N_{\exp}}} \tag{9}$$

Estimations of the precision index for I_0 = 830 and I_0 = 1100 W/m^2 with three air mass flow rates were calculated. The mean precision index of the experimental measurements in Figures 4 and 5 ranged between $2.80 \times 10^{-3} \leqslant S_{\overline{\eta}_{\exp}} \leqslant 7.75 \times 10^{-3}$. Meanwhile, deviations between the experimental results the theoretical predictions may be defined as:

$$E = \frac{1}{N_{\exp}} \sum_{i=1}^{N_{\exp}} \frac{\left|\eta_{theo,i} - \eta_{\exp,i}\right|}{\eta_{theo,i}} \times 100\% \tag{10}$$

where N_{exp}, $\eta_{theo,i}$ and $\eta_{exp,i}$ are the number of experimental measurements, theoretical predicted and experimental data of collector efficiencies, respectively. Accuracy deviations were calculated and shown in Table 1 within $1.33 \leqslant E \leqslant 9.32$ under two incident solar radiations I_0 for two configurations without (flat-plate type) and with attached wire mesh. It is seen that the experimental results fairly confirm the theoretical predictions, as indicated from Table 1. Comparisons between the theoretical predications and experimental results were achieved in good agreement, as observed from Figures 4 and 5.

Table 1. Deviations between the experimental results and theoretical predictions.

	$E = \frac{1}{N_{\mathbf{exp}}} \sum_{i=1}^{N_{\mathbf{exp}}} \frac{\left\|\eta_{theo,i} - \eta_{\mathbf{exp},i}\right\|}{\eta_{theo,i}} \times 100\%$			
	Flat-Plate Type		**Wire Mesh Packed**	
	I_0 (W/m^2)		I_0 (W/m^2)	
$\dot{m}$ (kg/h)	830	1100	830	1100
38.52	7.17	9.32	1.65	1.07
57.96	4.70	2.82	7.44	6.87
77.04	3.25	1.33	7.08	5.54

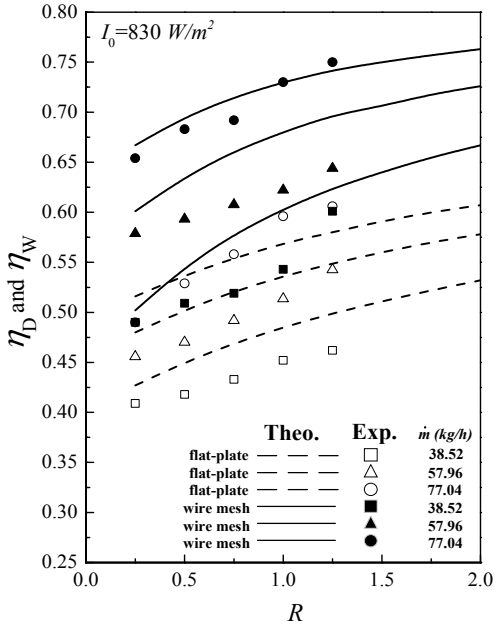

Figure 4. Effects of recycle ratio and air mass flow rate on collector efficiencies (I_0 = 830 W/m^2).

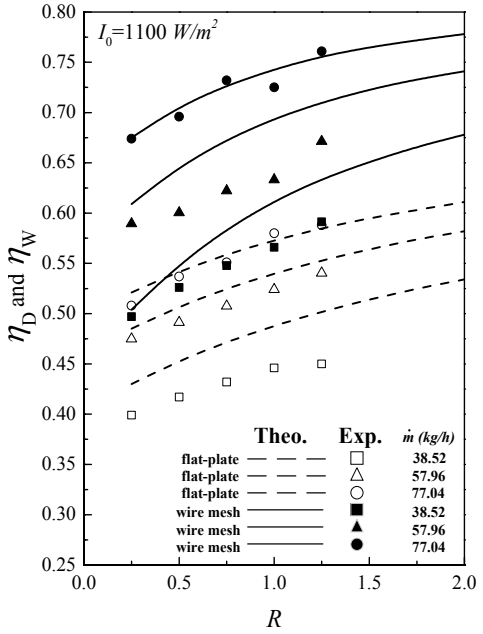

Figure 5. Effects of recycle ratio and air mass flow rate on collector efficiencies (I_0 = 1100 W/m^2).

Effects of recycle ratio and air mass flow rate on collector efficiencies, η_D and η_W, for both flat-plate type and wire mesh packed devices, respectively, are presented in Figures 4 and 5. Both collector efficiencies, η_D and η_W, increase with increasing recycle ratios and air mass flow rates owing to the air velocity enlargement, and thus, a higher convective heat transfer coefficient is achieved.

Collector performance improvements of I_D and I_W, for the flat-plate and wire mesh packed double-pass devices, respectively, under the same operating conditions with various incident solar radiations, air mass flow rates and recycle ratios as parameters are defined by the percentage increase in the collector efficiency compared to that in the downward single-pass device as follows:

$$I_D = \frac{\eta_D - \eta_S}{\eta_S} \times 100\% \quad (11)$$

$$I_W = \frac{\eta_W - \eta_S}{\eta_S} \times 100\% \quad (12)$$

Some calculated results are presented in Table 2.

Table 2. Theoretical predictions of heat-transfer efficiency improvement of I_D and I_W.

m (kg/h)	R	I_0 = 830 (W/m^2)		I_0 = 1100 (W/m^2)	
		Flat-Plate	Wire Mesh	Flat-Plate	Wire Mesh
		I_D (%)	I_W (%)	I_D (%)	I_W (%)
38.52	0.25	38.19	62.46	39.16	63.11
	0.5	45.63	76.38	46.60	77.67
	0.75	51.78	87.06	52.75	89.00
	1	56.96	95.15	57.93	98.06
	1.25	61.49	101.94	62.46	105.18
	1.5	65.37	107.12	66.34	110.68
	1.75	68.93	111.97	69.90	115.53
	2	72.17	115.86	72.82	119.42
57.96	0.25	29.73	62.43	31.08	64.59
	0.5	35.68	71.62	37.03	74.59
	0.75	40.81	78.65	41.89	81.89
	1	44.86	83.78	45.95	87.57
	1.25	48.38	88.38	49.46	91.89
	1.5	51.35	90.81	52.43	95.41
	1.75	54.05	94.05	55.14	98.11
	2	56.22	96.22	57.30	100.27
77.04	0.25	23.74	59.95	24.94	61.87
	0.5	28.78	66.67	29.98	69.31
	0.75	32.85	71.46	34.05	74.34
	1	36.45	75.06	37.41	78.18
	1.25	39.09	77.94	40.29	81.29
	1.5	41.73	79.86	42.69	83.45
	1.75	43.88	81.53	44.60	85.13
	2	45.56	82.97	46.52	86.57

The collector efficiency improvements increase with increasing recycle ratio but to a more remarkable extent with decreasing air mass flow rate. However, there is no significant influence of the incident solar radiation on the collector efficiency improvement. It is seen from Table 2 that the heat-transfer efficiency improvement of the wire mesh packed solar air heater is higher than that of the flat-plate type without attaching the wire mesh. The present work is actually the extension of the previous work [17] except for the different type of the external recycle. The graphical representation for comparisons with some experimental results and theoretical predictions obtained in [17] under the same design and operating parameters were illustrated to explain how the present device is preferred to be employed, as confirmed by Figure 6. This is the value and originality of the present device.

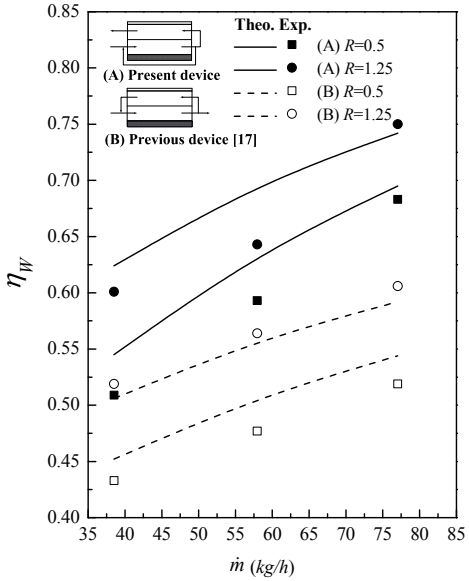

Figure 6. Comparisons of collector efficiency between the present device and the previous work (I_0 = 830 W/m^2).

The power consumption increment for the wire mesh packed devices I_P (P_S and P_W single-pass and double-pass devices, respectively) is defined by the percentage increase in the power consumption compared to that in the downward single-pass device [18,19]:

$$I_P = \frac{P_W - P_S}{P_S} \text{ for wire mesh packed solar air heaters} \quad (13)$$

The ratio I_W/I_P of both the collector efficiency improvement I_W and the power consumption increment I_P is illustrated to take into account both effect indexes for economic considerations in obtaining the suitable selections of the operating parameters. The results indicate the optimal ratio of I_W/I_P occurs at R = 0.5~1.0 for various mass flow rates, as indicated in Figure 7. It is of practical importance that applications of recycling operation and wire mesh packing for enhancing device performance of wire mesh packed solar air heaters is technically and economically feasible.

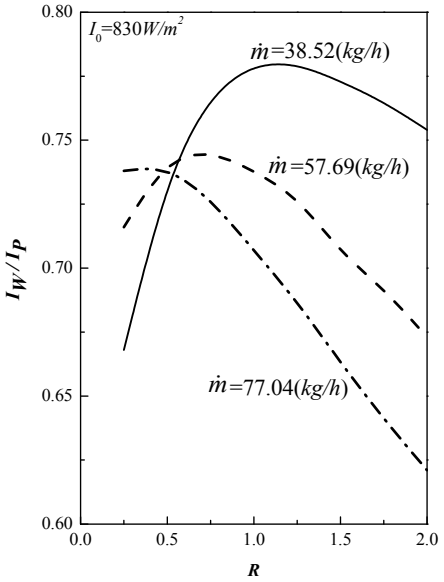

Figure 7. Effects of recycle ratio and air mass flow rate on the value of I_W/I_P.

5. Conclusions

The collector efficiency improvement in recycling double-pass solar air heaters with wire mesh packing have been developed analytically and experimentally. The comparisons of double-pass configurations with and without attaching a wire mesh were made to investigate the device performance improvement. The new design in the present study provides better collector efficiency due to the convective heat-transfer coefficient enhancement which the turbulent intensity created with the wire mesh attachment. The forgoing results can be summarized as follows: (1) With recycling operations and inserting a wire mesh, the collector efficiency increases with increasing recycle ratio R, incident solar radiation and air mass flow rates; (2) Collector performance improvements increase with increasing recycle ratio but with decreasing air mass flow rate, and no significant influence is found with respect to the incident solar radiation; (3) The optimal operating conditions for economic considerations of collector efficiency improvements with a relative small compensation of hydraulic dissipated energy increment were found at R = 0.5~1.0 for various mass flow rates; (4) the advantages of the present device are evident, and they will be an important contribution to the design of any particular application coupling external recycle and packing materials.

Acknowledgments: The authors wish to thank the Ministry of Science and Technology of the Republic of China for the financial support.

Author Contributions: This paper is a result of the full collaboration of all the authors. However, the concept for this research was conceived by Chii-Dong Ho, Chun-Sheng Lin contributed to mathematical derivations, Hsuan Chang and Yi-En Tien elaborated the manuscript preparation and Chun-Chieh Chao performed the experiments.

Conflicts of Interest: The authors declare no conflict of interest.

Nomenclature

A_c = surface area of the collector = LW (m^2)
C_p = specific heat of air at constant pressure (J/(kg· K))
E = deviation of the experimental measurements from theoretical predictions, defined in Equation (8)
h_a = convection coefficient between the bottom and lower subchannel ($W/m^2 \cdot K$)
h_b = convection coefficient between the absorber plate and upper subchannel ($W/m^2 \cdot K$)
$h_{r,p-c1}$ = radiation heat transfer coefficient between cover 1 and absorber plate ($W/m^2 \cdot K$)
$h_{r,p-R}$ = radiation heat transfer coefficient between absorber plate and bottom plate ($W/m^2 \cdot K$)
H = height of both upper and lower channels (m)
I_0 = incident solar radiation (W/m^2)
I_D = percentage of collector efficiency improvement in flat-plate air heater, defined in Equation (11)
I_W = collector efficiency improvement index, defined in Equation (12)
I_P = power consumption increment, defined in Equation (13)
L = channel length (m)
$\dot{m}$ = total air mass flow rate (kg/h)
N_{exp} = number of experimental measurements
P_D = power consumption of the double-pass air heater (W)
P_S = power consumption of downward-type single-pass device (W)
Q_u = useful energy gained by air (W)
R = recycle ratio
$S_{\eta_{\text{exp}}}$ = the precision index of an individual measurement
$S_{\overline{\eta}_{\text{exp}}}$ = the mean value of $S_{\eta_{\text{exp}}}$
$T_{a,i}$ = inlet air temperature (K)
$T_{a,0}$ = the mixing temperature of the subchannel a at x = 0 (K)
$T_{a,L}$ = the temperature of the subchannel a at x = L (K)

$T_{b,0}$ = the temperature of the subchannel b at x = 0 (K)
$T_{b,L}$ = the temperature of the subchannel b at x = L (K)
T_a = axial fluid temperature distribution in the lower subchannel (K)
T_b = axial fluid temperature distribution in the upper subchannel (K)
U_B = loss coefficient from the bottom of solar air heater to the ambient environment ($W/m^2 \cdot K$)
U_{B-s} = loss coefficient from the surfaces of edges and the bottom of the solar collector to the ambient environment ($W/m^2 \cdot K$)
U_{c1-s} = loss coefficient from the inner cover to the ambient environment ($W/m^2 \cdot K$)
U_T = loss coefficient from the top of solar air heater to the ambient environment ($W/m^2 \cdot K$)
W = width of both upper and lower subchannels (m)
z = axial coordinate (m)

Greek Letters

η_D = collector efficiency of the flat-plate double-pass device
η_S = collector efficiency of the downward type single-pass device
η_W = collector efficiency of the wire mesh packed solar air heater
$\eta_{\exp,i}$ = experimental data of collector efficiency
$\overline{\eta}_{\exp,i}$ = the mean value of the experimental data $\eta_{\exp,i}$
$\eta_{theo,i}$ = theoretical prediction of collector efficiency
ξ = dimensionless channel length

Appendix

$$B_1 = -W\left(h_b G_1 + h_b h_{r,p-c_1} G_1 G_4 - U_{c_1-s} h_b G_4\right)/R\dot{m}C_p \tag{A1}$$

$$B_2 = -W\left(h_b G_2 + h_b h_{r,p-c_1} G_2 G_4\right)/R\dot{m}C_p \tag{A2}$$

$$B_3 = -W\left(h_b G_3 + h_b h_{r,p-c_1} G_3 G_4\right)/R\dot{m}C_p \tag{A3}$$

$$B_4 = W\left(h_a G_6 + h_a h_{r,p-R} G_6 G_7\right)/(1+R)\,\dot{m}C_p \tag{A4}$$

$$B_5 = W\left(h_a G_5 + h_a h_{r,p-R} G_5 G_7 - U_{B-s} h_a G_7\right)/(1+R)\,\dot{m}C_p \tag{A5}$$

$$B_6 = W\left(h_a G_3 + h_a h_{r,p-R} G_3 G_7\right)/(1+R)\,\dot{m}C_p \tag{A6}$$

$$G_1 = -(h_a + U_T + U_B)/(U_T + U_B + h_a + h_b) \tag{A7}$$

$$G_2 = h_a/(U_T + U_B + h_a + h_b) \tag{A8}$$

$$G_3 = I_0 a_p \tau_g^2/(U_T + U_B + h_a + h_b) \tag{A9}$$

$$G_4 = (h_{r,p-c_1} + h_b + U_{c_1-s})^{-1} \tag{A10}$$

$$G_5 = -(h_b + U_T + U_B)/(U_T + U_B + h_a + h_b) \tag{A11}$$

$$G_6 = h_b/(U_T + U_B + h_a + h_b) \tag{A12}$$

$$G_7 = (h_{r,p-R} + h_a + U_{B-s})^{-1} \tag{A13}$$

$$Y_1 = \frac{(B_1 + B_5) + \sqrt{(B_1 - B_5)^2 + 4B_2B_4}}{2} \tag{A14}$$

$$Y_2 = \frac{(B_1 + B_5) - \sqrt{(B_1 - B_5)^2 + 4B_2B_4}}{2} \tag{A15}$$

$$C_1 = \frac{1}{F_1}\left[\frac{F_2 I_2 e^{Y_2} - B_4(F_2 - F_3)(1 + R - \mathrm{Re}^{Y_2})}{I_2 e^{Y_2}(1 + R - \mathrm{Re}^{Y_1}) - I_1 e^{Y_1}(1 + R - \mathrm{Re}^{Y_2})}\right] \tag{A16}$$

$$C_2 = -\frac{1}{F_1}\left[\frac{F_2 I_1 e^{Y_1} - B_4(F_2 - F_3)(1 + R - \mathrm{Re}^{Y_1})}{I_2 e^{Y_2}(1 + R - \mathrm{Re}^{Y_1}) - I_1 e^{Y_1}(1 + R - \mathrm{Re}^{Y_2})}\right] \quad \text{(A17)}$$

$$F_1 = B_1 B_5 - B_2 B_4 \quad \text{(A18)}$$

$$F_2 = B_3 B_4 - B_1 B_6 \quad \text{(A19)}$$

$$F_3 = B_2 B_6 - B_3 B_5 \quad \text{(A20)}$$

$$I_1 = Y_1 - B_4 - B_5 \quad \text{(A21)}$$

$$I_2 = Y_2 - B_4 - B_5 \quad \text{(A22)}$$

References

1. Razika, I.; Nabila, I.; Madani, B.; Zohra, H.F. The effects of volumetric flow rate and inclination angle on the performance of a solar thermal collector. *Energy Convers. Manag.* **2014**, *78*, 931–937. [CrossRef]
2. Al-Kayiem, H.H.; Yassen, T.A. On the natural convection heat transfer in a rectangular passage solar air heater. *Sol. Energy* **2015**, *112*, 310–318. [CrossRef]
3. El-Sebaii, A.A.; Al-Snani, H. Effect of selective coating on thermal performance of flat plate solar air heaters. *Energy* **2010**, *35*, 1820–1828. [CrossRef]
4. Vaziri, R.; Ilkan, M.; Egelioglu, F. Experimental performance of performance of perforated glazed solar air heaters and unglazed transpired solar air heater. *Sol. Energy* **2015**, *119*, 251–260. [CrossRef]
5. Kreith, F.; Kreider, J.F. *Principles of Solar Engineering*; McGraw-Hill: New York, NY, USA, 1978.
6. Duffie, J.A.; Beckman, W.A. *Solar Engineering of Thermal Processes*, 3rd ed.; Wiley: New York, NY, USA, 1980.
7. Gao, W.; Lin, W.; Liu, T.; Xia, C. Analytical and experimental studies on the thermal performance of cross-corrugated and flat-plate solar air heaters. *Appl. Energy* **2007**, *84*, 425–441. [CrossRef]
8. Ho, C.D.; Yeh, H.M.; Sheu, W.S. An analytical study of heat and mass transfer through a parallel-plate channel with recycle. *Int. J. Heat Mass Transfer* **1998**, *41*, 2589–2599. [CrossRef]
9. Ho, C.D.; Yang, W.Y. An analytical study of heat-transfer efficiency in laminar counterflow concentric circular tubes with external refluxes. *Chem. Eng. Sci.* **2003**, *58*, 1235–1250. [CrossRef]
10. Fudholi, A.; Sopian, K.; Ruslan, M.H.; Othman, M.Y.; Ruslan, M.H.; Bakhtyar, B. Energy analysis and improvement potential of finned double-pass solar collector. *Energy Convers. Manag.* **2013**, *75*, 234–240. [CrossRef]
11. Singh, S.; Dhiman, P. Recyclic double pass packed bed solar air heaters. *Int. J. Thermal Sci.* **2015**, *87*, 215–227.
12. Garg, H.P.; Sharma, V.K.; Bhargava, A.K. Theory of multiple-pass solar air heaters. *Energy* **1985**, *10*, 589–599. [CrossRef]
13. Wijeysundera, N.E.; Ah, L.L.; Tjioe, L.E. Thermal performance study of two-pass solar air heaters. *Sol. Energy* **1982**, *28*, 363–370. [CrossRef]
14. Ho, C.D.; Yeh, C.W.; Hsieh, S.M. Improvement in device performance of multi-pass flat-plate solar air heaters with external recycle. *Renew. Energy* **2005**, *30*, 1601–1621. [CrossRef]
15. Ho, C.D.; Yeh, H.M.; Wang, R.C. Heat-transfer enhancement in double-pass flat-plate solar air heaters with recycle. *Energy* **2005**, *30*, 2796–2817. [CrossRef]
16. Moffat, R.J. Describing the uncertainties in experimental results. *Exp. Therm. Fluid Sci.* **1988**, *1*, 3–17. [CrossRef]
17. Ho, C.D.; Lin, C.S.; Chuang, Y.C.; Chao, C.C. Performance improvement of wire mesh packed double-pass solar air heaters with external recycle. *Renew. Energy* **2013**, *57*, 479–489. [CrossRef]
18. Prasad, S.B.; Saini, J.S.; Singh, K.M. Investigation of heat transfer and friction characteristics of packed bed solar air heater using wire mesh as packing material. *Sol. Energy* **2009**, *83*, 773–783. [CrossRef]
19. Bird, R.B.; Stewart, W.E.; Lightfoot, E.N. *Transport Phenomena*, 2nd ed.; Wiley: New York, NY, USA, 2007.